Michelle L. Lamb,[†] Julian Tirado-Rives and William L. Jorgensen*

Department of Chemistry, Yale University, New Haven, CT 06520-8107, USA

Received 15 September 1998; accepted 2 November 1998

Abstract—A series of non-immunosuppressive inhibitors of FK506 binding protein (FKBP12) are investigated using Monte Carlo statistical mechanics simulations. These small molecules may serve as scaffolds for chemical inducers of protein dimerization, and have recently been found to have FKBP12-dependent neurotrophic activity. A linear response model was developed for estimation of absolute binding free energies based on changes in electrostatic and van der Waals energies and solvent-accessible surface areas, which are accumulated during simulations of bound and unbound ligands. With average errors of 0.5 kcal/mol, this method provides a relatively rapid way to screen the binding of ligands while retaining the structural information content of more rigorous free energy calculations.

Introduction

The binding protein of the immunosuppressant natural product FK506 (Fig. 1) has been the target of extensive investigation by both biochemical and theoretical techniques during the last 10 years. Discovery of the *cis-trans* peptidyl-prolyl isomerase (PPIase or rotamase) activity of FKBP12 (MW = 12 kDa) led to dissection of the rotamase mechanism[1–4] and hopes for the rapid design of low molecular weight immunosuppressant molecules that inhibited this activity. The crystal structure of FK506 bound to FKBP12 was crucial to this endeavor, as it demonstrated that the peptidomimetic α-ketoamide and pipecolyl portions of the ligand were buried but that much of the macrocycle remained exposed to solvent.[5] However, in later studies rotamase inhibition was found to be insufficient for immunosuppression; the FK506–FKBP12 complex associates with the surface of calcineurin (CN), a serine/threonine phosphatase, and hinders binding of subsequent proteins in the T-cell signaling pathway.[6] The "effector" region of FK506, which contacts CN, is opposite the α-ketoamide-pipecolic acid moiety.[7,8] Thus, the PPIase inhibitors developed through structure-based design efforts (e.g. compounds **1**–**7** in Table 1) formed a set of potential scaffolds for immunosuppressive effector components.[9,10]

Many of these non-immunosuppressive FKBP12 ligands are also able to promote neuronal growth in vitro and in vivo through binding to FKBP12.[11–13] Dose-response studies of neurite outgrowth in chick dorsal root ganglia resulted in an ED_{50} of 0.058 nM for compound **10**, for example.[11] In addition, tethered dimers of molecules similar to **4** have been used to "chemically-induce" dimerization[14] of targeted cellular proteins that had been adapted to include FKBP12 domains.[15] Modification of targets in appropriate signaling pathways can result in apoptosis or the induction of transcription; the prospects of this technology for gene therapy are intriguing.

Consequently, we have used theoretical techniques to probe this class of small molecules (Table 1) to gain insight into the physical basis for differences in FKBP12-binding activity and to evaluate new methods for the calculation of protein–ligand binding affinities. In previous work,[16] *relative* free energies of binding ($\Delta\Delta G_b$) for compounds **2**, **4**, and **8**–**10** were calculated by the free energy perturbation (FEP) technique using a Metropolis Monte Carlo (MC) algorithm for configurational sampling.[17] The parameters and geometry of one ligand were transformed into those of another with these simulations, both in solution and while bound to the protein. At each step of the transformation, the system was brought to equilibrium and the free energy difference relative to the previous step was computed. The difference in binding free energy for the two ligands was then found from the difference in the total free energy change for each (bound and unbound) transformation. While theoretically rigorous and accurate, calculations of this type are computationally demanding

Key words: Monte Carlo; linear response; FKBP12; rotamase inhibitors.

*Corresponding author. Fax: +203-432-6299; e-mail: bill@adrik.chem.yale.edu

[†] Current address: Dept. of Pharmaceutical Chemistry, University of California, San Francisco, Box 0446, San Francisco, CA 94143-0446.

0968-0896/99/$ - see front matter
PII: S0968-0896(99)00015-2

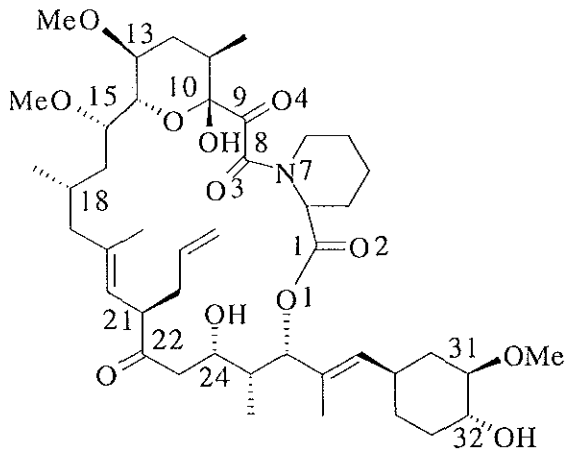

Figure 1. The immunosuppresent drug FK506.

and impractical for a large set of structurally diverse ligands.

An attractive alternative has emerged in linear interaction energy or linear response techniques (LR), as recently reviewed.[18] Unlike most FEP calculations, *absolute* free energies of binding (ΔG_b) for protein–ligand systems are estimated, and simulations of non-physical states (intermediate steps) are not required. In other respects, the molecular dynamics (MD) or MC simulation protocols are the same.

As first proposed, the linear interaction energy method employs eq (1) for the estimation of binding free energies.[19]

$$\Delta G_b = \beta\langle \Delta E^{Coulomb} \rangle + \alpha\langle \Delta E^{Lennard-Jones} \rangle \qquad (1)$$

These terms represent the change in interaction between a ligand and its environment (solvent and/or protein) upon binding. The electrostatic energy differences are obtained from average Coulombic interaction energies between the ligand and solvent ($E^{Coulomb}_{l-water}$) and the ligand and protein ($E^{Coulomb}_{l-FKBP}$) accumulated during simulations of the bound and unbound ligands. The Lennard–Jones (van der Waals) energy differences are found in an analogous manner. The original value of $\beta = 0.5$ is consistent with analyses of the response of polar solutions to changes in electric fields, such as the charging of an ion in water. Observed linear correlations between the molecular size (surface area, chain length) and solvation free energies of hydrocarbons suggested van der Waals interactions might respond linearly as well. A scale factor $\alpha = 0.161$ was obtained empirically from fitting to experimental binding data for a small set of endothiapepsin inhibitors.[19] Recently, Åqvist and co-workers have advocated the assignment of one of four reduced values of β according to the charge-state or polarity of the ligand and have obtained an appropriate value for α by fitting to data for a larger set of protein–ligand pairs.[20–22] An extended linear response equation,[23,24] in which a cavitation term based on solvent-accessible surface areas (SASA) is added and all parameters are empirically determined, is given in eq (2) below. This model was first applied to the calculation of free energies

Table 1. FKBP12 inhibitors[a]

	Compound	$K_{i,app}$, nM
1	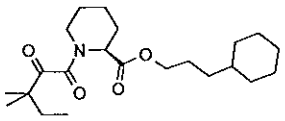	186, 170[b]
2	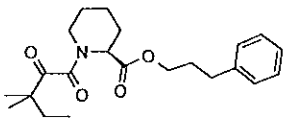	110, 250[b]
3	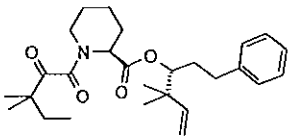	250
4	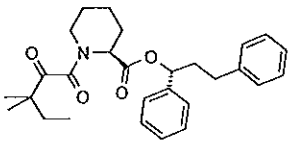	10, 17[b]
5	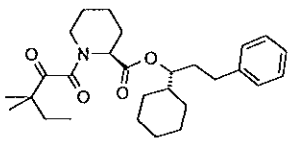	7
6	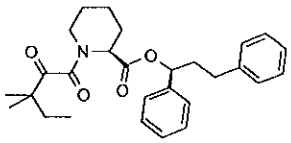	300–600
7	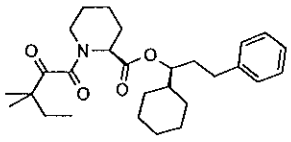	300
8	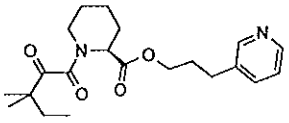	165, 130[b]
9	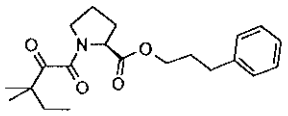	42[b]
10	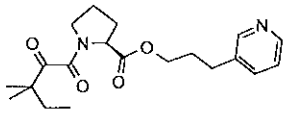	7.5[b]
11	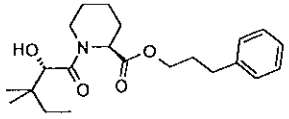	2300[c]

[a]Rotamase inhibition data taken from refs 9 and 10 unless otherwise noted.
[b]Data from ref 11.

scale factors to $\beta = 0.131$, $\alpha = 0.131$ and $\gamma = 0.014$ yielded acceptable estimates of thrombin-binding affinity as well.[25] In addition, the extended linear response equation has potential for predictions of other properties important for pharmacological activity, such as the estimation of ligand lipophilicity.[24] It has been observed that the contribution of the ΔSASA term is often nearly constant, so the case in which the simple addition of a constant improves the fit has also been considered [eq (3)].[20,25]

$$\Delta G_b = \beta\langle\Delta E^{Coulomb}\rangle + \alpha\langle\Delta E^{Lennard\text{-}Jones}\rangle + \gamma\langle\Delta SASA\rangle \quad (2)$$

$$\Delta G_b = \beta\langle\Delta E^{Coulomb}\rangle + \alpha\langle\Delta E^{Lennard\text{-}Jones}\rangle + \gamma \quad (3)$$

In contrast to most proteins studied previously with this technique, FKBP12 has a distinctly hydrophobic binding pocket lined with aromatic residues, and only two intermolecular hydrogen bonds are observed in the crystal structure of inhibitor **4** with the protein.[9] Consequently, it was expected that the electrostatic behavior of these molecules might deviate from linear response and that the van der Waals contributions to binding might be larger than previously observed for other systems. To determine the suitability of the linear response approximation for binding to FKBP12, MC simulations of the bound and unbound states for all 11 inhibitors in Table 1 were performed.

Computational Details

The modeling strategy employed here was consistent with the FEP study described previously,[16] based on the 4-FKBP12 crystal structure (1FKG)[9] and the OPLS force field.[26–28] (A full listing of parameters for these molecules may be found in ref 29) The first five inhibitors were easily built from **4**. Atoms of the 1-phenyl substituent were simply removed to obtain **2**, and for compound **1**, a united-atom cyclohexyl group[30] was positioned in the plane of the original 3-phenyl ring. The vinyl group of **3** was also represented with united-atom parameters and was positioned at the minimum of the $CH3{-}C{-}CH{=}CH_2$ torsional energy profile (180.0°) and aligned with an edge of the 1-phenyl ring of **4**.[29] One side of this ring was within 3.2 Å of His^{87} and Tyr^{82}, while the other was positioned more than 3.5 Å from Phe^{46} and Glu^{54}. Accordingly, the orientation which maximized hydrophobic contact between the protein and **3** was chosen. Inhibitor **5** incorporated the crystal structure orientations of the cyclohexyl and *tert*-pentyl groups from **5**-FKBP12 (1FKH).[9] In **1** and **5**, the cyclohexyl groups were treated as rigid units, as were all ligand and protein aromatic groups. It was thought that the conformational flexibility within the rings of these substituents would be less important to binding than the overall flexibility of the ligand, and thus sampling was focused accordingly. Starting geometries for the unbound ligand simulations were taken from these initial bound conformations.

All simulations were performed using the MCPRO

The ligands and protein–ligand complexes were solvated with 22 Å spheres of TIP4P water molecules. First, 1×10^6 (1 *M*) configurations of water-only equilibration with preferential sampling of molecules close to the inhibitor was performed, followed by 16 *M* configurations of sampling of the entire system with all solvent molecules sampled uniformly. Next, data was collected for 8 *M* configurations averaged in blocks of 2×10^5 configurations. To ensure convergence, averaging for all unbound ligands was extended to 16 *M* configurations.

To obtain protein-bound structures of **6** and **7**, the final conformations of **4** and **5** above were epimerized within the FKBP12 binding pocket via a slow perturbation protocol. Eight sequential double-wide windows with $\Delta\lambda = 10.0625$ were used. In each window, 4 *M* configurations were sampled to slowly transform between the two ligands in an energetically reasonable way. This procedure was repeated with the free ligands in solution. The simulations of ligands **8**–**11** were started from the final structures of FEP simulations reported previously.[16,29] In each case, energy components were averaged over 8 *M* (bound) and 16 *M* (unbound) configurations of the system.

As was mentioned above, the initial structure for **2** had been generated from the bound conformation of **4** with the 1-phenyl atoms removed. Following an FEP calculation from **4** to **2**, further sampling was carried out within the first windows of both a phenyl→pyridyl FEP[16] and a carbonyl→hydroxyl FEP.[29] The final conformations of these windows were then used to start two additional linear response MC simulations, **2a** and **2b**, respectively. These additional data points provide one gauge of precision.

Solvent-accessible surface areas for the ligands in both aqueous and protein environments were calculated using the SAVOL2 program.[32] This algorithm has been incorporated into MCPRO, and the necessary atomic radii are calculated from the corresponding OPLS σ parameters via 1/2 ($2^{1/6}\sigma$). Using the standard solvent radius for water, 1.4 Å, the SASAs of the ligands were calculated for the structure at the end of each block of MC configurations and were averaged.

Average energy and solvent-accessible surface area differences were fit to the experimental binding data (Table 1) to obtain linear response parameters α, β, and γ according to eqs (1)–(3). This procedure was performed with a Simplex-based algorithm. As inhibition data for the majority of the ligands in this set has been reported by Holt and co-workers,[9,10] in cases where two values have been measured the values from these authors were used for fitting.

Results and Discussion

Average intermolecular energy components and SASAs

Each ligand and protein–ligand complex was solvated with a sphere of explicit water molecules and sampled as

ligand SASAs accumulated during the simulations are reported in Table 2. As has been observed with thrombin inhibitors, the ligand–solvent Coulombic energy components, $E^{Coulomb}_{l-water}$, fluctuate the most during the simulations.[25] However, both the magnitude of the energy contribution and the magnitude of the fluctuation are reduced compared to the positively charged or zwitterionic protease inhibitors, as expected for the neutral ligands of this set. All of the ligands in solution have undergone hydrophobic collapse relative to their bound conformations but to differing extents, as significant flexibility is observed in the propyl side chain. The Lennard–Jones interactions for the α-ketoamide molecules in solution scale generally with molecular size; **1** and **2** (and **8–10**) have the least favorable average energies, followed by compound **3**, and finally there is a small range of energies for **4–7**. The solvent accessible surface area of amide carbonyl O3 is generally ca. 10 Å^2 less than that of the keto (O4) or ester (O2) atoms, and usually only one water molecule is found to interact with this atom. This is consistent with molecular dynamics results for *trans*-FK506.[29] Often, O4 interacts strongly with one water molecule (H-O4 distance, ca. 1.8 Å), while a second molecule hovers 0.5 Å further away. Also, water molecules are found to interact with the faces of aromatic rings. In the case of **2**, an unusual long-lived solvation pattern is noted. The water molecule that hydrogen bonds to O3 further associates with one directed into the center of the less-accessible face of the phenyl ring (Fig. 2).

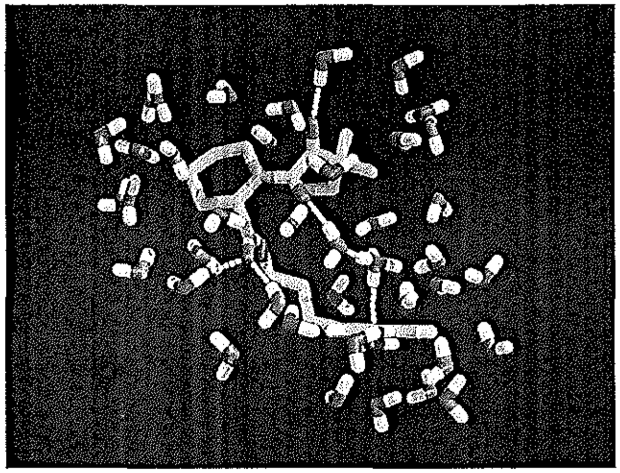

Figure 2. The hydrogen bonding network in **2**, with waters that bridge between the amide O3 and phenyl ring.

Typical of many FKBP12-ligand complexes,[33] the crystal structure of 4-FKBP12 contains contacts between O4 and aromatic hydrogens of Tyr[26], Phe[36], and Phe[99], with the pipecolyl ring sitting over Trp[59].[9] The 3-phenylpropyl moiety binds in the solvent-exposed FK506-cyclohexyl groove of FKBP12 between Ile[56] and Tyr[82], and these residues form hydrogen bonds with the ester and amide carbonyl oxygens of the ligand. The 1-phenyl substituent interacts with Phe[46] and the tertiary pentyl group of the inhibitor. The two crystallographic intermolecular hydrogen bonds are maintained throughout all of the FKBP12-ligand simulations, and none of the ligands deviates significantly from the original orientation

Table 2. Average interaction energies (kcal/mol) and solvent-accessible surface areas of the inhibitors (Å^2) from the aqueous and FKBP12 MC simulations[a]

Compound	$E^{Coulomb}_{l-water}$	$E^{L-J}_{l-water}$	$E^{Coulomb}_{l-FKBP}$	E^{L-J}_{l-FKBP}	SASA[b]
1 aq	−23.16(0.32)	−35.96(0.15)			665.4(1.2)
1FKBP	−0.24(0.15)	−15.09(0.12)	−19.14(0.16)	−39.53(0.14)	202.1(1.6)
2 aq	−31.28(0.46)	−34.59(0.21)			653.9(1.9)
2a aq	−29.91(0.35)	−33.90(0.16)			629.3(2.3)
2b aq	−27.11(0.38)	−33.26(0.16)			620.6(2.3)
2FKBP	−5.15(0.31)	−13.74(0.09)	−19.73(0.21)	−40.29(0.13)	202.9(5.1)
2aFKBP	−2.14(0.19)	−13.99(0.12)	−21.56(0.16)	−38.01(0.17)	222.4(6.8)
2bFKBP	−1.62(0.19)	−13.95(0.14)	−20.97(0.20)	−37.92(0.21)	188.6(7.0)
3 aq	−27.68(0.36)	−36.52(0.16)			680.9(1.2)
3FBKP	−1.41(0.20)	−15.31(0.13)	−21.15(0.20)	−44.06(0.15)	221.2(3.0)
4 aq	−31.89(0.42)	−39.63(0.22)			715.1(1.4)
4FKBP	−5.30(0.38)	−17.84(0.11)	−21.25(0.15)	−42.73(0.19)	248.8(2.5)
5 aq	−28.43(0.50)	−40.12(0.19)			728.3(1.8)
5FKBP	−6.49(0.19)	−16.54(0.10)	−20.58(0.14)	−44.00(0.16)	244.9(2.1)
6 aq	−32.84(0.55)	−38.35(0.12)			712.2(1.6)
6FBKP	−8.00(0.19)	−18.10(0.13)	−17.26(0.15)	−38.46(0.20)	232.4(3.0)
7 aq	−29.64(0.34)	−38.48(0.15)			688.3(1.9)
7FKBP	−3.92(0.23)	−16.10(0.15)	−17.09(0.18)	−43.65(0.21)	282.3(7.1)
8 aq	−30.53(0.43)	−32.75(0.18)			618.4(1.8)
8FBKP	−13.51(0.48)	−12.03(0.15)	−18.03(0.16)	−38.80(0.19)	176.0(4.7)
9 aq	−29.88(0.50)	−31.67(0.17)			624.9(2.2)
9FBKP	−1.43(0.19)	−14.04(0.09)	−23.59(0.16)	−39.40(0.17)	179.3(6.4)
10 aq	−33.45(0.40)	−32.89(0.22)			630.8(2.2)
10FKBP	−11.95(0.31)	−12.82(0.10)	−20.02(0.18)	−38.77(0.15)	183.2(6.5)
11 aq	−42.57(0.43)	−31.24(0.21)			626.7(1.4)
11FKBP	−2.72(0.34)	−15.19(0.10)	−18.23(0.15)	−38.61(0.13)	185.5(4.4)

[a]The standard error of the means is given in parentheses.

of 4. In general, the aromatic rings of the inhibitors are oriented perpendicularly to the ring of Tyr[82], although a clearly T-shaped interaction is not dominant. Consistent with the hydrophobic binding pocket, the largest contribution to the protein–ligand interaction energy in all cases comes from the Lennard–Jones terms. In addition, the most favorable van der Waals interactions with FKBP12 are observed for the more hydrophobic **3**, **5**, and **7** compared to their more aromatic or smaller counterparts.

An estimate of the precision of the simulations was determined from the three simulations of **2** in solution. One model was derived directly from the **4**-FKBP12 crystal structure, while the others (**2a** and **2b**) were obtained through earlier FEP simulations from **4**. In solution, there is a 4 kcal/mol range in the $E^{Coulomb}_{l-water}$ components and a 2 kcal/mol range in $E^{L-J}_{l-water}$. Variations among the average energy components reported for all simulations of **2**-FKBP12 are on the order of 2–3 kcal/mol. It must be noted that the terms from simulations **2a** and **2b** are more similar to each other than to those from the original **2** simulation.

As energy and SASA *differences* between the protein and aqueous environments are the quantities that are scaled to estimate binding affinity, these values are recorded in Table 3. Two of the lowest affinity inhibitors, **3** and **11** have the largest van der Waals energy differences between bound and unbound ligands. Ligands **6**, **7**, and **11** have the most unfavorable $\Delta E^{Coulomb}$, while only **8** has a net favorable electrostatic interaction upon binding. Approximately 450 Å^2 of each ligand is buried upon binding to FKBP12. This represents 65% of the surface of inhibitor **4**, for example. The largest change is noted for inhibitors **5** and **6** (ca. 480 Å^2 buried), while the smallest difference is found for **7** (ca. 410 Å^2).

Optimization of the LR equations

The energies and surface areas of Table 2 were used first with previously determined scaling parameters to compute FKBP12-binding affinities. The original parameters of Åqvist[19] do not describe binding to this protein well at all; the free energies of binding are underestimated with an average unsigned error ($<|error|>$) of 9.3 kcal/mol. Results with the thrombin-derived parameters are of more appropriate magnitude (−9.3 (**5**) to −6.3 (**11**) kcal/mol, $<|error|> = 1.4$ kcal/mol), although both the set of atomic radii for SASAs and the all-atom representation of the thrombin inhibitors differed from the study presented here. However, to improve the correspondence with experiment for FKBP12, new values for α, β, and γ were found by fitting the average energy and surface area differences to the experimental binding free energies. The results for the various models investigated are summarized in Table 4.

The first step was to employ eq (1) with $\beta = 0.5$ and derive an appropriate value for α, as was done originally for endothiapepsin.[19] This model resulted in $\alpha = 0.626$ and yielded free energies which deviated significantly from experiment. In particular, the maximum unsigned error for model 1 was 4.4 kcal/mol, which diminishes its predictive value given that the range of experimental binding affinities is 3.4 kcal/mol. Furthermore, compound **3**, a poor inhibitor, was predicted to bind as well as the highest affinity ligand, **8**.

As expected, the linear response assumption for electrostatic energies, $\beta = 0.5$, does not appear to hold well for binding to FKBP12. When the value of β is set based on ligand composition[20] and α derived empirically with eq (1) (model 2) or both β and α treated as free parameters (model 3), average unsigned error and RMS to experiment were improved but the maximum errors are still greater than 2kcal/mol. With model 2, the α-ketoamide ligands required $\beta = 0.43$; **11** called for $\beta = 0.37$ due to its single hydroxyl substituent.[20]

Fitting the data with three parameters yielded an RMS deviation of 0.7 kcal/mol, whether or not the SASA difference was included explicitly (eq (2) versus eq (3)). Values of $\beta = 0.139$, $\alpha = 0.194$, and $\gamma = 0.0145$ (model 4) ranked the ligands in a qualitatively reasonable way

Table 3. Calculated energy and surface-area differences[a] with representative binding affinities

Compound	$\Delta E^{Coulomb}$	ΔE^{L-J}	ΔSASA	ΔG_b, kcal/mol			
				model 2	model 4	model 6	expt[b]
1	3.8	−18.7	−463.3	−9.6	−9.8	9.7	−9.2(−9.2)
2	6.4	−19.4	−451.0	−8.9	−9.4	−9.4	−9.5(−9.0)
2a	6.2	−18.1	−406.9	−8.2	−8.5	−8.6	−9.5(−9.0)
2b	4.5	−18.6	−432.0	−9.2	−9.2	−9.3	−9.5(−9.0)
3	5.1	−22.7	−459.7	−11.5	−10.4	(−10.9)[c]	−9.0
4	5.3	−20.9	−466.3	−10.2	−10.1	−10.3	−10.9(−10.6)
5	1.4	−20.4	−483.4	−11.6	−10.8	−10.9	−11.1
6	7.6	−18.2	−479.8	−7.6	−9.4	−9.0	−8.7[d]
7	8.6	−21.3	−406.0	−9.0	−8.8	−9.3	−8.9
8	−1.0	−18.1	−442.4	−11.3	−10.1	−10.2	−9.2(−9.4)
9	4.8	−21.8	−445.6	−11.0	−10.0	−10.5	−10.1
10	1.5	−18.7	−447.6	−10.6	−9.9	−10.0	−11.1
11	21.6	−22.6	−441.2	−5.5	−7.8	−7.8	−7.7

[a]Units: kcal/mol and Å^2, respectively.
[b]References given in notes to Table 1, $\Delta G = RT ln K_i$.
[c]Compound **3** not included in the derivation of this model.

DOCKET ALARM

Explore Litigation Insights

Docket Alarm provides insights to develop a more informed litigation strategy and the peace of mind of knowing you're on top of things.

Real-Time Litigation Alerts

Keep your litigation team up-to-date with **real-time alerts** and advanced team management tools built for the enterprise, all while greatly reducing PACER spend.

Our comprehensive service means we can handle Federal, State, and Administrative courts across the country.

Advanced Docket Research

With over 230 million records, Docket Alarm's cloud-native docket research platform finds what other services can't. Coverage includes Federal, State, plus PTAB, TTAB, ITC and NLRB decisions, all in one place.

Identify arguments that have been successful in the past with full text, pinpoint searching. Link to case law cited within any court document via Fastcase.

Analytics At Your Fingertips

Learn what happened the last time a particular judge, opposing counsel or company faced cases similar to yours.

Advanced out-of-the-box PTAB and TTAB analytics are always at your fingertips.

API

Docket Alarm offers a powerful API (application programming interface) to developers that want to integrate case filings into their apps.

LAW FIRMS
Build custom dashboards for your attorneys and clients with live data direct from the court.

Automate many repetitive legal tasks like conflict checks, document management, and marketing.

FINANCIAL INSTITUTIONS
Litigation and bankruptcy checks for companies and debtors.

E-DISCOVERY AND LEGAL VENDORS
Sync your system to PACER to automate legal marketing.